Energy Loss Triggered by Atomic-Scale Lateral Force

Filippo Federici Canova,[1,2,*] Shigeki Kawai,[3,†] Christian de Capitani,[4] Ken-ichi Kan'no,[5] Thilo Glatzel,[3]
Bartosz Such,[3] Adam S. Foster,[2] and Ernst Meyer[3]

[1]*Department of Physics, Tampere University of Technology, P.O. Box 692, FI-33010 Tampere, Finland*
[2]*COMP, Department of Applied Physics, Aalto School of Science, P.O. Box 11100, FI-00076 Aalto, Finland*
[3]*Department of Physics, University of Basel, Klingelbergstrasse 82, CH-4056 Basel, Switzerland*
[4]*Institute of Mineralogy and Petrography, University of Basel, Bernoullistrasse 30, CH-4056 Basel, Switzerland*
[5]*Department of Material Science and Chemistry, Wakayama University, Wakayama 640-8510, Japan*
(Received 5 February 2013; published 16 May 2013)

We perform bimodal atomic force microscopy measurements on a Br-doped NaCl (001) surface to investigate the mechanisms behind frequency shift and energy dissipation contrasts. The peculiar pattern of the dissipated energy in the torsional channel, related to frictional processes, is increased at the positions of Br impurities, otherwise indistinguishable from Cl ions in the other measured channels. Our simulations reveal how the energy dissipates by the rearrangement of the tip apex and how the process is ultimately governed by lateral forces. Even the slightest change in lateral forces, induced by the presence of a Br impurity, is enough to trigger the apex reconstruction more often, thus increasing the dissipation contrast; the predicted dissipation pattern and magnitude are in good quantitative agreement with the measurements.

Friction, wear, and adhesion are some of the most fundamental processes in nature [1,2]. Characterization and control of such phenomena are of key importance in every kind of machinery [3,4], as well as biological systems at different scales [5]. The dynamics of any two objects rubbed against each other is ultimately governed by atomic-scale interactions between the microscopic asperities that build up the effective contact area [6]. Since the invention of atomic force microscopy in 1986 [7], a detailed study of friction and wear properties became possible by reducing the contact area down to the nanometer scale [8], and a large amount of scientific effort has been directed towards understanding the ''nanoscale'' origin of friction [9–13]. It has been shown that the classical laws often fail at this scale: Friction has indeed a complex dependence on the applied load [14], sliding velocity [15], and temperature [16]; several studies investigated how friction can be controlled [2,17], and the existence of a frictionless regime was also proven [18,19]. Although these measurements have successfully shed light on some aspects of the nanoscale nature of friction, we still lack detailed knowledge of the atomic-scale processes measured with a controlled single atomic contact. In particular, the link between frictional and adhesive forces, and dissipated energy at the atomic scale, remains poorly explored. While normal and lateral forces can be associated to the gradient of the interaction potential [20], their relation to nonconservative and adhesive mechanisms is yet unknown.

Dynamic force microscopy (DFM) enables us to measure the tip-sample forces normal to the surface by detecting changes in the oscillation frequency shift Δf_Z of a stiff

cantilever [21], yielding high sensitivity and preventing jump-into-contact instability. This technique has been widely used to characterize insulating materials [22,23]. Furthermore, the tip-sample interaction potential can then be extracted from the measured Z-distance-dependent curve of Δf_Z [24]. If the gradient is calculated along the surface plane, one can estimate lateral forces as well [20,25–27]. However, this method cannot take into account nonconservative effects happening during the lateral tip movement and their influence on the extracted forces. Alternatively, one can excite the torsional resonance of the cantilever (TR-AFM) [28,29], enabling direct detection of the lateral force gradient from the torsional frequency shift, Δf_{TR} [30], and the energy loss in the oscillation E_{TR} from the driving excitation signal. Since the tip oscillates laterally thousands of times while acquiring a sample, the signal gives an average value, equivalent to the measurement of several friction loops in contact mode, and the dissipated energy corresponds to the average energy loss in the loops. Operating at dithering amplitude below the surface lattice size ($A_{TR} < 100$ pm) enables us to measure atomic-scale lateral interactions, and the instabilities responsible for friction losses can be detected on the surface with atomic resolution.

The flexural and torsional modes can also be combined in the so-called bimodal operation [31–33] allowing simultaneous measurement of both normal and lateral interactions, with all the advantages of dynamic atomic force microscopy (AFM): In particular, it is possible to measure accurately lateral interactions at relatively close distance through the torsional signals, while the vertical tip-sample distance is controlled by the flexural frequency shift, giving

higher accuracy than the normal deflection control in conventional friction force microscopy. Unfortunately, this method further complicates the interpretation of the data, because only a small part of the torsional oscillation will take place when the tip is close to the surface, in the lower turning point of the flexural cycle, while for most of the time, the tip is further away, subject to weaker interactions.

Despite the extreme sensitivity of DFM, damping images cannot be routinely analyzed, since the underlying dissipative mechanisms are still not experimentally accessible and, therefore, remain unknown. Different theoretical studies suggest the main cause of dissipation to be the adhesion hysteresis [34,35]; however, its atomic-scale detail is strongly dependent on the particular system [36–39]. Therefore, theoretical calculations become important to provide understanding of the imaging mechanism in terms of the atomic motion.

In this Letter, we study the Br-doped NaCl(001) surface by combining different experimental as well as theoretical techniques. We measure the tip-sample interactions by using bimodal DFM and study the dissipative mechanism behind the peculiar pattern observed in E_{TR} maps: First, we formulate a general mathematical model explaining the results and carry out molecular dynamics simulations. The assumptions of the mathematical model were validated by our atomistic calculations, and the effects of Br defects in the images were also predicted and understood.

The studied sample consists of a Br-doped NaCl crystal ($NaCl_{0.9}Br_{0.1}$). The concentration of Br was *ex situ* analyzed with energy dispersive x-ray spectroscopy (see Supplemental Material [40] for details). The DFM experiments were performed with our homemade ultrahigh vacuum apparatus, operating at room temperature [41]; the tip was indented into the sample prior the measurements. Vertical and lateral tip-sample interactions were measured by using bimodal DFM from the flexural and torsional resonance frequency shifts of a commercially available Si cantilever [42–44]. The frequency shifts of both flexural Δf_Z and torsional modes Δf_{TR} were detected with two sets of the digital phase-locked loop (Nanonis: dual-OC4), and the amplitudes (A_Z and A_{TR}) were kept constant by controlling the excitation signals to the dither piezoelectric actuator; from the excitation signals, the vertical E_Z and lateral E_{TR} energy dissipations were obtained [45]. Further details on the experiments are described in the Supplemental Material [40].

Figure 1 shows simultaneous measurements of the frequency shifts Δf and the energy dissipation E for both modes, measured at quasiconstant height: The measured topographic contrast is as small as 1 pm, thus below the sensitivity of the digital electronics. The Δf_Z, Δf_{TR}, and E_Z maps reveal the well-known atomic pattern of NaCl (001): As a result of the large flexural amplitude, the Δf_Z contrast is weak and noisy, while the Δf_{TR} signal, affected only by lateral site-dependent interactions [44], gives very
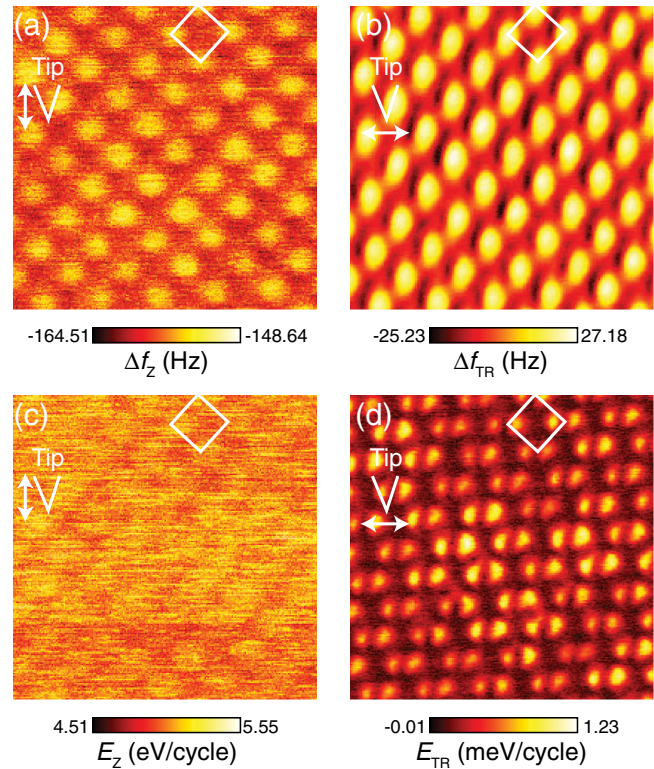
FIG. 1 (color online). Simultaneous measurements of (a) Δf_Z, (b) Δf_{TR}, (c) E_Z, and (d) E_{TR} maps of NaCl:Br (001) at a quasiconstant height. Measurement parameters: $\Delta f_Z = -150$ Hz, $f_Z = 154800$ Hz, $A_Z = 15$ nm, $Q_Z = 31032$, $f_{TR} = 1484136$ Hz, $A_{TR} = 50$ pm, $Q_{TR} = 176891$, and bias voltage $V = -2.621$ V.

high resolution [42,43]. The overall magnitude of the energy dissipation in the flexural mode E_Z is quite large (≈ 4.5 eV), and it systematically increases as the tip-sample distance is reduced (see Fig. 4S in the Supplemental Material [40] for more details); the atomic contrast in E_Z map is weak but anyway visible on top of the large offset. This behavior is consistent with the mechanical coupling issue [46,47].

Our attention was quickly drawn to the E_{TR} map, whose pattern seems inconsistent with the crystal lattice: The observed contrast features do not correspond to the surface cation or anion sites. Two distinct dissipation peaks are measured, with a slight asymmetry in relative intensity, adjacent to the negative surface ions, with a local minimum located above the atomic site; despite their small intensity (<1.21 meV/cycle), these features are sharply resolved and have a clear contrast. Interestingly, about 20% of these double features have a brighter contrast than the others, suggesting that they result from Br impurities. The concentration of impurities in the E_{TR} map appears higher than the value given by energy dispersive x-ray spectra, and we attribute this effect to the segregation and diffusion of Br ions during annealing. Unlike previous experiments on mixed crystals where the Br impurities could be seen with conventional noncontact-AFM topography [48] or

energy dissipation [49], in our experiment Br and Cl can be distinguished only by the increased E_{TR} contrast of the double feature: This remarks the delicate dependence of the contrast mechanism on the atomic detail of the tip.

Figure 2(a) shows the Δf_{TR} and E_{TR} maps in a narrow area of the surface, including both Cl and Br, while the details of the analyzed line scan are shown in Fig. 2(b). The shoulder observed in Δf_{TR} next to the negative ions is the tail of the features coming from the Cl and Br ions on the adjacent atomic rows and is due to the small angle between the tip dithering direction, along the fast-scan direction, and the crystal orientation. Along A-A' and B-B', two-dimensional distance-dependent measurements of Δf_{TR} and E_{TR} were performed, and, from those, the actual lateral force gradient F'_x and dissipation $E_{lateral}$ at a constant tip-sample separation were extracted, thus removing the averaging effect due to the large flexural oscillation amplitude (see Supplemental Material [40] for details). Figure 2(c) shows the extracted lateral force gradient F'_x and energy dissipation $E_{lateral}$: The lateral force gradient at

FIG. 2 (color online). (a) Simultaneous measurements of Δf_{TR} and E_{TR} maps of Br-doped NaCl(001). (b) Corresponding line profiles along A-A' and B-B'. (c) Extracted two-dimensional maps of lateral force gradient F'_x and lateral energy dissipation $E_{lateral}$ via the measured Δf_{TR} and E_{TR}, measured along A-A' and B-B'.

the negative ion sites is around -2 N/m, and the lateral energy dissipation is up to 40 meV/cycle. The negative sign of the force gradient above Cl and Br is a quite puzzling result, which suggests an attractive tip-surface interaction at the Cl and Br sites: This is in contrast with Δf_Z maps, that imply a repulsive tip-sample interaction on the very same sites. The data indicate that the tip apex changes polarity at close approach due to a reversible instability; thus, the lateral oscillation detects the inverted interaction.

Using a very simple model, we can already grasp the origin of the double peak in E_{TR}. If we assume the tip-sample interaction potential along an atomic row to be given by $V_{TS}(x) = \cos(2\pi x/a)$, where a is the lattice constant, the potential has its extrema at $x = 0$, $a/2$, where the ions are located. Then the lateral force is obtained from its gradient: $F_x(x) = -\nabla_x V_{TS}(x) \propto \sin(2\pi x/a)$; this approximates the electrostatic potential between the surface and a single-ion tip reasonably well, as shown in the Supplemental Material [40]. The lateral force is strongest at $x = \pm a/4$, or rather between positive and negative ions along the atomic row, and under such intense forces the tip apex might reconfigure itself, as suggested in Ref. [35], ultimately leading to hysteresis during the oscillation cycle and energy dissipation to appear as a double feature.

We performed classical molecular dynamics simulations of the lateral tip movement in order to confirm the existence of such a reconstruction mechanism and predict how much dissipation it could account for. The model treats atoms as point charges interacting through Coulomb electrostatic and short-range Buckingham-type pair potentials [50–52]. The AFM tip is modeled dynamically, following a procedure similar to the experiment, where a rough oxide tip indents the NaCl sample, adsorbing surface material at the apex [39]. Furthermore, the tip is annealed through several flexural AFM oscillation cycles, until the apex reconstructs into a crystallinelike shape [Fig. 3(a), inset]. The clean surface model consists of a $10 \times 10 \times 4$ NaCl slab, and the doped model was obtained by replacing a surface Cl atom with Br. The boundary atoms of the slab, as well as the uppermost layers of the tip, are harmonically restrained and a thermostat keeps them at 300 K, while all other atoms are Newtonian. The simulation features only the torsional oscillation of the tip, at constant height with an amplitude $A_{TR} = 0.5$ Å: The cycle is always initiated with a random phase, thus taking into account the incommensurable flexural and lateral frequencies. The lateral force and dissipation are then obtained by averaging forces on the tip atoms and their hysteresis over 100 simulated cycles at a constant tip-sample distance of $z = 3.5$ Å; the calculation is repeated by using different initial tip positions above the surface, covering the area of a unit cell (more details in the Supplemental Material [40]).

A possible dominant factor in the dissipation energy in the flexural oscillation, namely, the formation and rupture of atomic chains [39], was proven to be prohibited by this
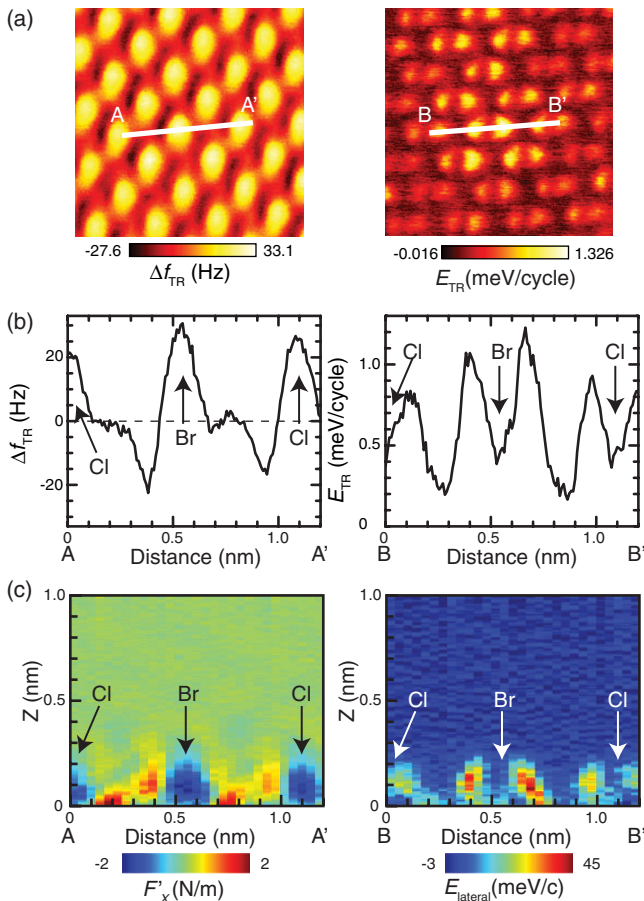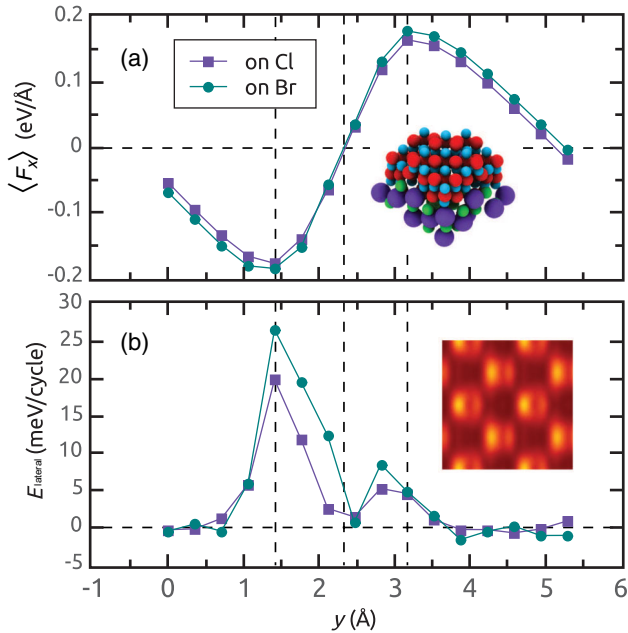
FIG. 3 (color online).   (a) Average lateral force calculated along an atomic row with either Cl (purple squares) or Br (green circles) as the middle atom; the inset shows the model tip with the MgO holder (cyan and red atoms) and the annealed NaCl apex (green and purple atoms). (b) Energy dissipation along the same scan line obtained from the average hysteresis in constant-height oscillation cycles; the inset shows the simulated dissipation image.

tip; furthermore, the Cl-terminated apex is repelled by surface Cl and Br atoms due to their Coulomb interaction, and thus we expect the same Δf_Z pattern seen in the experiments: This has been verified and the calculated force curves are shown in the Supplemental Material [40]. Figure 3(a) shows the lateral force calculated along atomic lines with either Cl or Br atoms at the midpoint: There is no significant difference with respect to the negative ion, and this agrees with the lack of contrast on Br defects in the experimental Δf_{TR} map. The force gradient on the negative ion is 4 N/m. In Fig. 3(b), energy dissipation is observed at the points where lateral forces reach their highest values, and from the atomic trajectories we can see how this is caused by small stochastic reconstructions of the apex. After computing a few more points on parallel scan lines, it was possible to reconstruct a dissipation image [Fig. 3(b), inset]. The simulated pattern and the dissipation value are in good agreement with the extracted lateral dissipation $E_{lateral}$ from the experiments. There is a clear asymmetry in the relative intensity of the two peaks, also observed, to a lesser degree, in the experimental images. The model tip is not symmetric with respect to the scan direction; thus, apex reconstructions are more likely to occur on one side of the negative surface ion. Dissipation calculated on the surface containing Br impurities is clearly higher, and this can be due to the Br ion remaining on average 7.5 pm above the surface plane and pushing the neighboring Na atoms away by 7–8 pm with

respect to their positions in the clean NaCl surface, hence interacting more strongly with the tip, and triggering more reconstruction events. The measured Δf_z contrast, combined with the increased dissipation on Br defects and the symmetry of the surface, suggests that the Cl and Br ions are located at the center of the double peaks and that the tip should be negatively terminated (details in the Supplemental Material [40]).

In conclusion, we found that energy dissipation in the torsional oscillation is caused by atomic reconstruction of the tip apex under strong lateral forces resulting from the interaction with the surface. The structural changes are triggered at the points of highest forces, located between positive and negative surface ions along an atomic row: The initial theoretical hypothesis was confirmed by more elaborate molecular dynamics simulations with a realistic model tip. The apparently odd dissipation pattern observed in the experiment was reproduced in our simulations with good quantitative agreement, considering the simplicity of the classical model. Strikingly, the small variation in the tip-sample interaction, caused by the presence of Br impurities, not detectable by the conservative Δf signals at room temperature, was observed in the E_{TR} signal as an increased dissipation contrast. With our simulations we could attribute this effect to the higher vertical position of Br impurities and the locally stretched lattice of the neighboring Na atoms: Despite such changes consisting of only a few picometer displacements, they are enough to increase the occurrence rate of apex reconstructions, and hence dissipation, and result in a clearly visible increase in contrast.

Our study gives unambiguous evidence of how extremely small variations in the surface structure, undetectable by conventional DFM, produce a distinct signature in the lateral dissipation signal, where these small changes amplify the nonconservative interaction. Furthermore, our contribution shows how DFM energy dissipation, often considered a by-product of the measurement apparatus, provides unique insight into the surface properties: The observed subatomic dissipation features correspond to the atomic-scale energy loss in an ultrasmall friction loop. Apart from studying the ultimate friction processes, this technique can be used to image and identify hidden defects or the bond stiffness between a surface and adsorbed molecules, that might be of crucial importance in novel technological applications.

*filippo.federici@tut.fi

†shigeki.kawai@unibas.ch

[1] B. N. J. Person, *Sliding Friction, Physical Principles and Applications* (Springer, Berlin, 2000), 2nd ed.

[2] R. W. Carpick, Science **313**, 184 (2006).

[3] W. Wang, Y. Wang, H. Bao, B. Xiong, and M. Bao, Sens. Actuators A **97–98**, 486 (2002).

[4] *Friction and Wear in Machinery* (American Society of Mechanical Engineers, New York, 1964), Vol. 16.

[5] V. Bormuth, V. Varga, J. Howard, and E. Schäffer, Science **325**, 870 (2009).

[6] J. Archard, Wear **113**, 3 (1986).

[7] G. Binnig, C. F. Quate, and C. Gerber, Phys. Rev. Lett. **56**, 930 (1986).

[8] C. M. Mate, G. M. McClelland, R. Erlandsson, and S. Chiang, Phys. Rev. Lett. **59**, 1942 (1987).

[9] C. Mate, R. Erlandsson, G. M. McClelland, and S. Chiang, Surf. Sci. **208**, 473 (1989).

[10] E. Gnecco, R. Bennewitz, T. Gyalog, and E. Meyer, J. Phys. Condens. Matter **13**, R619 (2001).

[11] H. Hölscher, D. Ebeling, and U. D. Schwarz, Phys. Rev. Lett. **101**, 246105 (2008).

[12] Q. Li, T. E. Tullis, D. Goldsby, and R. W. Carpick, Nature (London) **480**, 233 (2011).

[13] J. S. Choi, J.-S. Kim, I.-S. Byun, D. H. Lee, M. J. Lee, B. H. Park, C. Lee, D. Yoon, H. Cheong, K. H. Lee, Y.-W. Son, J. Y. Park, and M. Salmeron, Science **333**, 607 (2011).

[14] N. Sasaki, M. Tsukada, S. Fujisawa, Y. Sugawara, S. Morita, and K. Kobayashi, Phys. Rev. B **57**, 3785 (1998).

[15] E. Gnecco, R. Bennewitz, T. Gyalog, C. Loppacher, M. Bammerlin, E. Meyer, and H. J. Guntherodt, Phys. Rev. Lett. **84**, 1172 (2000).

[16] Z. Tshiprut, S. Zelner, and M. Urbakh, Phys. Rev. Lett. **102**, 136102 (2009).

[17] A. Socoliuc, E. Gnecco, S. Maier, O. Pfeiffer, A. Baratoff, R. Bennewitz, and E. Meyer, Science **313**, 207 (2006).

[18] A. Socoliuc, R. Bennewitz, E. Gnecco, and E. Meyer, Phys. Rev. Lett. **92**, 134301 (2004).

[19] M. Dienwiebel, G. S. Verhoeven, N. Pradeep, J. W. M. Frenken, J. A. Heimberg, and H. W. Zandbergen, Phys. Rev. Lett. **92**, 126101 (2004).

[20] A. Schwarz, H. Hölscher, S. M. Langkat, and R. Wiesendanger, AIP Conf. Proc. **696**, 68 (2003).

[21] T. R. Albrecht, P. Grütter, D. Horne, and D. Rugar, J. Appl. Phys. **69**, 668 (1991).

[22] S. Morita, F. J. Giessibl, and R. Wiesendanger, *Noncontact Atomic Force Microscopy* (Springer, Berlin, 2009), Vol. 2.

[23] C. Barth, A. S. Foster, C. R. Henry, and A. L. Shluger, Adv. Mater. **23**, 477 (2011).

[24] M. A. Lantz, H. J. Hug, R. Hoffmann, P. J. A. van Schendel, P. Kappenberger, S. Martin, A. Baratoff, and H. J. Güntherodt, Science **291**, 2580 (2001).

[25] A. Schirmeisen, D. Weiner, and H. Fuchs, Phys. Rev. Lett. **97**, 136101 (2006).

[26] M. Ternes, C. P. Lutz, C. F. Hirjibehedin, F. J. Giessibl, and A. J. Heinrich, Science **319**, 1066 (2008).

[27] B. J. Albers, T. C. Schwendemann, M. Z. Baykara, N. Pilet, M. Liebmann, E. I. Altman, and U. D. Schwarz, Nat. Nanotechnol. **4**, 307 (2009).

[28] O. Pfeiffer, R. Bennewitz, A. Baratoff, E. Meyer, and P. Grütter, Phys. Rev. B **65**, 161403 (2002).

[29] M. Reinstädler, U. Rabe, V. Scherer, and U. Hartmann, Appl. Phys. Lett. **82**, 2604 (2003).

[30] S. Kawai, N. Sasaki, and H. Kawakatsu, Phys. Rev. B **79**, 195412 (2009).

[31] N. F. Martinez, S. Patil, J. R. Lozano, and R. García, Appl. Phys. Lett. **89**, 153115 (2006).

[32] J. R. Lozano and R. García, Phys. Rev. Lett. **100**, 076102 (2008).

[33] S. Kawai, T. Glatzel, S. Koch, B. Such, A. Baratoff, and E. Meyer, Phys. Rev. Lett. **103**, 220801 (2009).

[34] B. Gotsmann, C. Seidel, B. Anczykowski, and H. Fuchs, Phys. Rev. B **60**, 11051 (1999).

[35] N. Sasaki and M. Tsukada, Jpn. J. Appl. Phys. **39**, L1334 (2000).

[36] L. N. Kantorovich and T. Trevethan, Phys. Rev. Lett. **93**, 236102 (2004).

[37] S. A. Ghasemi, S. Goedecker, A. Baratoff, T. Lenosky, E. Meyer, and H. J. Hug, Phys. Rev. Lett. **100**, 236106 (2008).

[38] F. Federici Canova and A. S. Foster, Nanotechnology **22**, 045702 (2011).

[39] S. Kawai, F. Federici Canova, T. Glatzel, A. S. Foster, and E. Meyer, Phys. Rev. B **84**, 115415 (2011).

[40] See Supplemental Material at http://link.aps.org/supplemental/10.1103/PhysRevLett.110.203203 for additional experimental and theoretical details.

[41] L. Howald, E. Meyer, R. Lüthi, H. Haefke, R. Overney, H. Rudin, and H. J. Güntherodt, Appl. Phys. Lett. **63**, 117 (1993).

[42] S. Kawai, T. Glatzel, S. Koch, B. Such, A. Baratoff, and E. Meyer, Phys. Rev. B **81**, 085420 (2010).

[43] S. Kawai, R. Pawlak, T. Glatzel, and E. Meyer, Phys. Rev. B **84**, 085429 (2011).

[44] S. Kawai, F. Federici Canova, T. Glatzel, T. Hynninen, E. Meyer, and A. S. Foster, Phys. Rev. Lett. **109**, 146101 (2012).

[45] B. Anczykowski, B. Gotsmann, H. Fuchs, J. P. Cleveland, and V. B. Elings, Appl. Surf. Sci. **140**, 376 (1999).

[46] A. Labuda, Y. Miyahara, L. Cockins, and P. H. Grütter, Phys. Rev. B **84**, 125433 (2011).

[47] S. Kawai, T. Glatzel, B. Such, S. Koch, A. Baratoff, and E. Meyer, Phys. Rev. B **86**, 245419 (2012).

[48] R. Bennewitz, O. Pfeiffer, S. Schär, V. Barwich, E. Meyer, and L. Kantorovich, Appl. Surf. Sci. **188**, 232 (2002).

[49] R. Bennewitz, S. Schär, E. Gnecco, O. Pfeiffer, M. Bammerlin, and E. Meyer, Appl. Phys. A **78**, 837 (2004).

[50] R. A. Buckingham, Proc. R. Soc. A **168**, 264 (1938).

[51] A. L. Shluger, A. L. Rohl, D. H. Gay, and R. T. Williams, J. Phys. Condens. Matter **6**, 1825 (1994).

[52] A. I. Livshits, A. L. Shluger, A. L. Rohl, and A. S. Foster, Phys. Rev. B **59**, 2436 (1999).